CHILDHOOD MEDULLOBLASTOMA DIAGNOSIS USING MULTISCALE FRAMEWORK

Vishal Eswaran
Department of Information Technology and Management,
University of Texas Dallas,
Dallas, USA.
vishalspost@gmail.com

Usha Eswaran
Society of Innovative Educationalist and Scientific Research Professional Chennai,
California University FCE,
California, USA.
drushaaeswaran@gmail.com

Submitted: *Jun, 18, 2022* ***Revised:*** *Aug, 27, 2022* ***Accepted:*** *Sep, 10, 2022*

Abstract: This paper proposes an efficient Shearlet Based Childhood MedulloBlastoma (SBCMB) detection system. It is a classification system that extracts prominent characteristics for childhood MedulloBlastoma diagnosis from a given collection of histopathological images. Then, those extracted features are used with specific decision-making algorithms to categorize the histopathological images. After representing the histopathological images by Shearlet, a multiscale framework, Improved Sequential Forward Selection (ISFS) algorithm, is employed to select the dominant feature subset. Finally, Multi-Layer Perceptron (MLP) with ten hidden layers is utilized for melanoma classification. Based on the results of the evaluation of the SBCM system, it seems that the classification may be accomplished exclusively by the ISFS-based features and that the accuracy of the classifier depends on these selected features. The SBCM system provides 97.62% accuracy on 10x magnified images and 98.77% on 100x magnified images for childhood MedulloBlastoma diagnosis.

Keywords: MedulloBlastoma, computerized diagnosis, multiscale framework, histopathological images.

I. INTRODUCTION

Histopathological evaluation of removed MedulloBlastoma (MB) tumour specimens was the only approach that was ever used in the past for the purpose of grading MB. The World Health Organization (WHO) categorized Tumors as Grade I from IV. The grading of MB reflects the level of histological divergence that exists between the tumour and the cells from which it originated. Due to the MB cell's cytological malignant, necrosis-prone looks, all other grade tumours are associated with grade IV tumours.

The survey presented in this section provides a comparison foundation that can be used to assess the performance of the newly developed approach. In addition, it has been observed that the challenge of determining which method is the most effective for a specific application is becoming progressively more difficult. Furthermore, the absence of a universally accepted experimental protocol further complicates the evaluation of different algorithms.

The cascading approach in [1] combines the advantages of deep learning approaches with methods of textural analysis features. First, it uses three deep-

learning Convolutional Neural Networks (CNNs) to extract deep-learning spatial characteristics. Then, it uses Discrete Wavelet Transform (DWT) to extract time-frequency characteristics. Finally, it creates a time-efficient computer-aided diagnosis system by fusing these features with the help of the discrete cosine transform and the Principal Component Analysis (PCA). Transfer learning is employed in [2] for childhood MB diagnosis. It provides a complete categorization of MB tumours. An in-depth analysis of EfficientNets is performed for childhood MB classification. The same deep learning network is employed in [3] for childhood MB classification of histopathological images.

The categorization of MB samples is carried out in [4] for both the binary and the multiclass categories. Two transfer learning networks, Alexnet and Visual Geometry Group (VGG), are trained for feature extraction, and the Softmax function is utilized as the classifier for both networks. In addition, their performances are compared with Support Vector Machine (SVM). A single-layer neural network is utilized in [5] for MB classification using gene expression instead of histopathological images.

A composite deep learning architecture is described in [6] for MB classification. DWT-based texture analysis reduces the dimension of fused features from ten CNNs. A bi-directional long-short-term memory network is used for the categorization of histopathological images. An improvement in sub-type identification is obtained in [7] by combining textural analysis with deep learning approaches. In addition to the original histopathological images, three cutting-edge deep-learning models are trained with textural images created from two different texture analysis methods. The spatial and textural information within the images enables the system to perform better.

Two distinct CNN models are utilized in [8] for analyzing their performances in MB classification. The first CNN has 16 layers and is developed by the VGG. The second network has only two layers. Both CNNs are visual feature extractors of a histopathological image to classify anaplastic and non-anaplastic MB tumours. Magnetic resonance features are employed in [9] to classify childhood brain tumours. The multi-parametric characteristics are classified using SVM and quantum-enhanced SVM algorithms.

The architectural characteristic and the distribution of cells are the two important features that support the framework in [10] for automatic categorization. The feature set includes five texture characteristics from the intensity-based features, such as co-occurrence and run length features, first-order histogram, and binary patterns with the Tamura features. Fivefold cross-validation is used for performance evaluation with the classifiers such as SVM, decision tree, and nearest neighbour classifier with PCA as a feature reduction approach. Different texture features such as Laws, Haralick, and Haar have been employed in [11] for histological image classification to diagnose MB. It uses random forest ensembles to categorize histological images into anaplastic or non-anaplastic.

In this paper, an efficient SBCMB detection system is proposed. It uses Shearlets and MLP for the classification of histopathological images. Shearlets are a multiscale framework that enables effective encoding of anisotropic properties and is introduced for analyzing sparse representations. Section 2 discusses the flow of the proposed SBCMB system, and their performances are evaluated in the next section using two different magnified ($10x$ and $100x$) histopathological images. The final section provides the conclusion based on the results of the proposed SBCMB system.

III. PROPOSED SYSTEM

The classification of dermoscopic images is possible if the appropriate characteristics are chosen and a suitable algorithm for making decisions is used. Nevertheless, this is a challenging process since it is extremely difficult to analyze the patterns, and the choice of the input data is also reliant on the domain. Figure 1 shows the proposed SBCMB detection system.

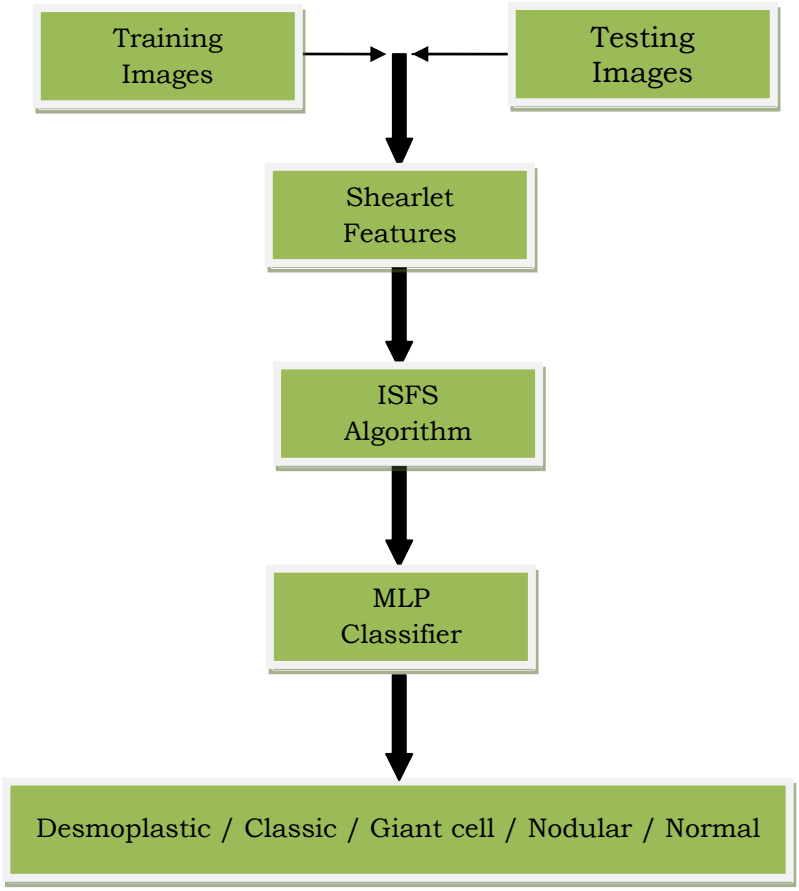

Fig. 1 Block diagram of the proposed SBCMB detection system

A. Shearlets

Though many transformations such as Wavelet, Curvelet, and Contourlet have been designed recently, Shearlet has more advantages in detecting texture features. When an image is decomposed using a wavelet, a condensed expression of the images is obtained, which contains a greater abundance of coefficients with low values. However, they are unable to represent the information in multi-directional. To represent multi-directional, directional filter banks are utilized, and many transformations, such as Curvelet, Contourlet, and Shearlet, are developed.

Since Curvelet was initially intended for use in the continuous domain, it is very challenging to implement directly in the discrete domain. Contourlet may be thought of as a discrete domain Curvelet transform. It is superior to the wavelet regarding the number of directional components or sub-bands provided at

each scale. Both the Curvelet and Contourlet are used to extract the location of the border curves, but only in smooth areas. On the other hand, shearlet can recognize curves even in regions that aren't perfectly smooth [12]. As a result, the Shearlet is used as a method for the extraction of features for skin cancer diagnosis. It is defined as

$$\psi_{ast}(x) = \left|\det M_{as}\right|^{-\frac{1}{2}} \Psi(M_{as}^{-1}(x-t)) \quad (1)$$

where scale (a), shear (s), and translation (t). M_{as} are the product of shear and dilation matrices. The frequency domain of the Shearlet is shown in Figure 2.

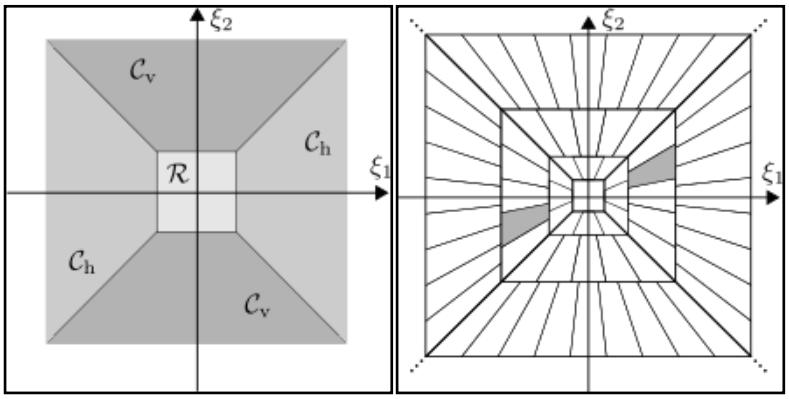

Fig. 2 Frequency domain by Shearlet

B. Selection of Dominant Characteristics

The accuracy of classification and regression algorithms depends on how groups of features perform together. This is true regardless of whether the analysis is performed on raw or simulated data. Also, the contribution of each feature is dependent on the feature subset to which it is added or from which it is removed. In addition to this, because the same observation also applies to the potential higher-order feature interdependencies and the significance of individual feature subsets, Therefore, an effective search algorithm ought to have the flexibility to "find" complete subsets, which, if incorporated, might potentially lead to increased performance to or removed from the feature subset that is presently being investigated (search state) [13]. The flexibility of the search increases in proportion to the number of pathways permitted between states.

A random search is likely not valid; therefore, more organized techniques are needed while retaining flexibility. All of the different subset search algorithms utilize a standard search quadruple. The proposed system develops an ISFS algorithm for this purpose. It begins in a condition that is first considered to be empty sets. It then continues to the feature subset that has the most outstanding performance after evaluating all of the parent states of the current state, which is equivalent to adding one feature. It will end when the addition of traits can no longer increase performance. In non-nested subsets, when the best subset at complexity 1 is not necessarily a subset of the best subset at complexity N, the selection can miss the optimum subset. This happens, particularly in situations with qualities that depend on one another. For this reason, it is best to let ISFS run until the whole complement of functionality has been implemented.

C. Multilayer Perceptron

Figure 3 shows a Feed Forward Neural Network (FFNN). Adding a hidden layer provides the non-linearity in the system with adaptive weights and a differentiable activation function [14]. This gives the network the ability to learn and adapt to its environment. In most cases, the back-propagation technique is used to train these types of networks. This algorithm optimizes a mean-squared error function during training.

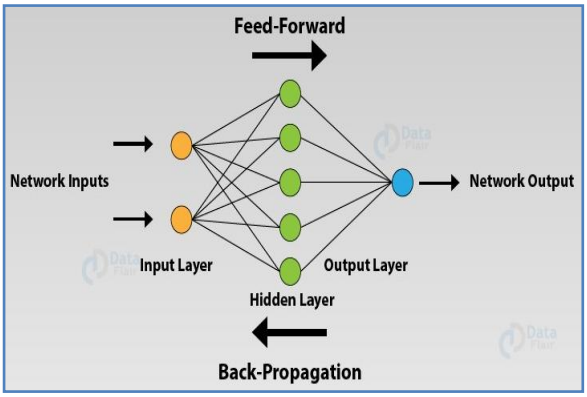

Fig. 3 Architecture of FFNN

The learning rule (Widrow-Hoff) is used throughout the training process for the layer of adaptive weights responsible for linking the output node through the hidden layer. The gradient of the error function is determined by the chain rule that connects the input nodes to the hidden layer. It is possible for the error surfaces of MLPs to include local minima, which in most cases prohibit gradient descent algorithms. However, local minima only sometimes guarantee greater generalization than less optimum solutions.

III. RESULTS AND DISCUSSIONS

The SBCMB classification method designed in the previous section is evaluated using 202 histopathology images retrieved from [15]. Histopathological images magnified into 10x and 100x are included in this collection. These images are categorized into five groups: desmoplastic, classic, giant cell, nodular, and normal. The resolution of the histopathology image magnified by ten times is 2048 by 1536 pixels, but the resolution of the image magnified by 100 times is just 800 by 600 pixels. The number of images used in the performance analysis of the SBCMB classification system is shown in Figure 4. Figure 5 and Figure 6 shows samples images of 10x magnified and 100x magnified respectively.

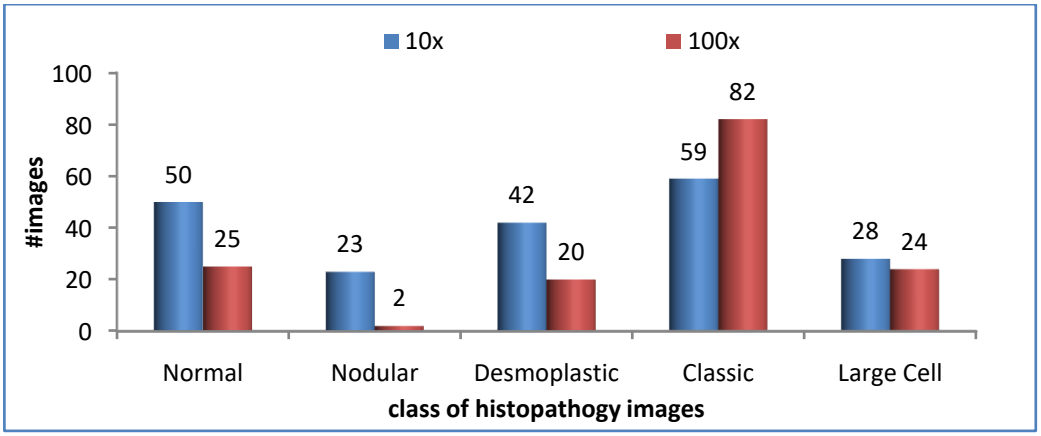

Fig. 4 Number of images available in both magnification (10x and 100x)

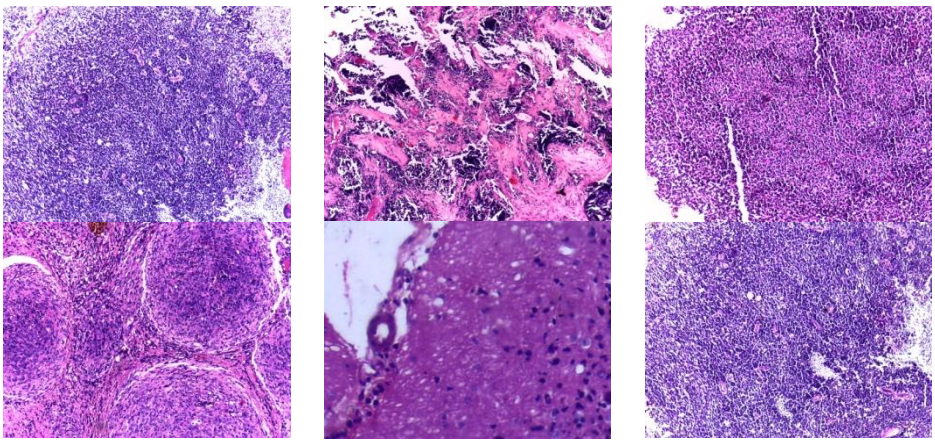

Fig. 5 Sample images magnified at 10x

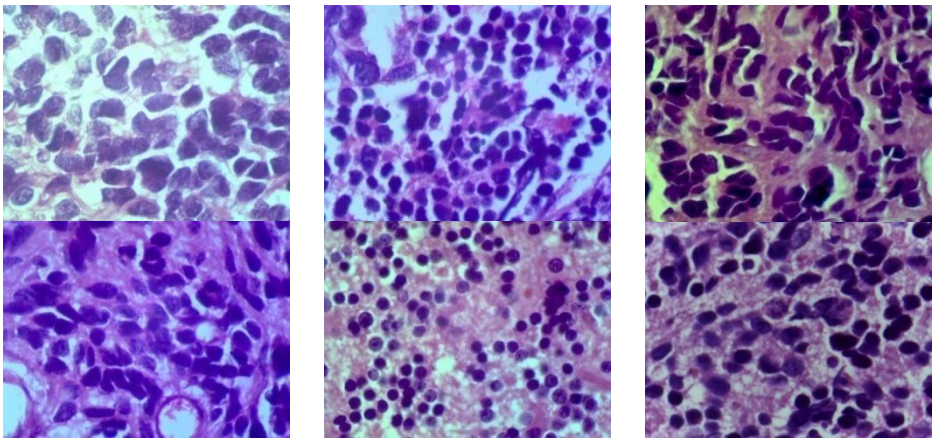

Fig. 6 Sample images magnified at 100x

Table 1 lists the several assessment metrics that are often used in the medial domain. These metrics are derived based on the number of true classifications (i.e., those that are accurate) and false classifications (those that are erroneous) of normal and abnormal images. In Table 1, T_P is a True Positive, F_N is False Negative, T_N is True Negative, and F_P is False Positive.

TABLE. 1 Performance metrics used

Accuracy	Sensitivity	Specificity
$\frac{T_P + T_N}{T_P + F_P + T_N + F_N}$	$\frac{T_P}{T_P + F_N}$	$\frac{T_N}{T_N + F_P}$

The performance of the proposed SBSC system on the 10x magnified images is shown in Table 2 by changing the decomposition levels, and Table 3 shows the performance on the 100x magnified images.

TABLE. 2 Results of the proposed SBCMB detection system on 10x magnified images

level	Accuracy (%)	Sensitivity (%)	Specificity (%)
1	84.28	75.62	87.7
2	90.95	86.45	92.84
3	97.62	97.28	97.98
4	92.95	89.78	94.37
5	90.95	86.45	92.98

TABLE. 3 Results of the proposed SBCMB detection system on 100x magnified images

level	Accuracy (%)	Sensitivity (%)	Specificity (%)
1	86.43	77.77	89.85
2	93.1	88.6	94.99
3	98.77	98.43	99.13
4	95.1	91.93	96.52
5	93.1	88.6	95.13

It is observed from Table 2 and Table 3 that the subset features selected from the 3rd level Shearlet by the ISFS method have the highest accuracy of 97.62% and 98.77% on 10x and 100x images. To analyze the ISFS feature selection approach, the system is also tested without feature selection. Figure 7 shows the obtained accuracy using ISFS and without ISFS. It can be seen from Figure 7 that the ISFS approach improves the performance of the SBSC detection system by more than 12% accuracy.

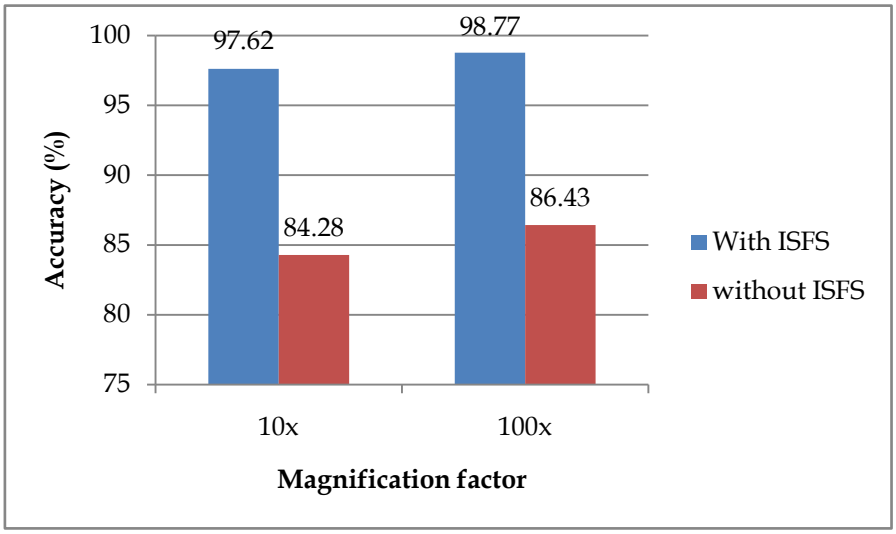

Fig. 7 Performance of ISFS approach on 10x and 100x magnified images

IV. CONCLUSIONS

This paper presented an efficient SBCMB detection system for the problem of childhood MedulloBlastoma diagnosis. A new framework for feature selection is introduced, known as ISFS. The goal of feature selection is not to find a single optimal combination of characteristics but instead sets of feature subsets that are not dominated by any other combination of characteristics. Even in the most straightforward scenario, feature selection entails at least two goals: the maximization of the model's performance and the minimization of the cardinality of the features that make up the subset. Results proved that the SBCMB system performance is improved when using the feature subsets from ISFS. The proposed SBCMB system gives a good result with 97.28% sensitivity and 97.98% specificity on 10x images and 98.43% sensitivity and 99.13% specificity on 100x magnified images.

Funding Statement: The authors received no specific funding for this study.

Conflicts of Interest: The authors declare that they have no conflicts of interest to report regarding the present study.

REFERENCES

[1]. O. Attallah, "MB-AI-His: histopathological diagnosis of pediatric medulloblastoma and its subtypes via AI," Diagnostics, vol. 11, no. 2, 2021, pp. 1-26.

[2]. M. Bengs, M. Bockmayr, U. Schüller and A. Schlaefer, "Multiscale Input Strategies for Medulloblastoma Tumor Classification using Deep Transfer Learning," Current Directions in Biomedical Engineering, vol. 7, no. 1, 2021, pp. 1-4.

[3]. C. M. Bhuma and R. Kongara, "Childhood Medulloblastoma Classification Using EfficientNets," IEEE Bombay Section Signature Conference, 2020, pp. 64-68.

[4]. D. Das, L. B. Mahanta, B. K. Baishya and S. Ahmed, "Classification of Childhood Medulloblastoma and its subtypes using Transfer Learning features - A Comparative Study of Deep Convolutional Neural Networks," International Conference on Computer, Electrical & Communication Engineering, 2020, pp. 1-5.

[5]. A. Narayanan, E. Nana and E. Keedwell, "Analyzing gene expression data for childhood medulloblastoma survival with artificial neural networks," Symposium on Computational Intelligence in Bioinformatics and Computational Biology, 2004, pp. 9-16.

[6]. O. Attallah, "CoMB-deep: composite deep learning-based pipeline for classifying childhood medulloblastoma and its classes," Frontiers in neuroinformatics, 2021, vol. 21, pp. 1-19.

[7]. O. Attallah and S. Zaghlool, "AI-Based Pipeline for Classifying Pediatric Medulloblastoma Using Histopathological and Textural Images," Life, vol. 12, no. 2, 2022, pp. 1-17.

[8]. A. Cruz-Roa, J. Arévalo, A. Judkins, A. Madabhushi and F. González, "A method for medulloblastoma tumor differentiation based on convolutional neural networks and transfer learning," 11th International Symposium on Medical Information Processing and Analysis, vol. 9681, 2015, pp. 8-15.

[9]. E. Akpınar, N. M. Duc and B. Kesercİ, "The Role of Quantum-enhanced Support Vector Machine using Multi-parametric MRI Parameters in Differentiating Medulloblastoma from Ependymoma," IEEE International Conference on Quantum Computing and Engineering, 2022, pp. 882-885.

[10]. D. Das, L. B. Mahanta, S. Ahmed and B. K. Baishya, "Classification of childhood medulloblastoma into WHO ‐ defined multiple subtypes based on textural analysis," Journal of microscopy, vol. 279, no. 1, 2020, pp. 26-38.

[11]. Y. Lai, S. Viswanath, J. Baccon, D. Ellison, A. R. Judkins and A. Madabhusai, "A texture-based classifier to discriminate anaplastic from non-anaplastic medulloblastoma," 37th Annual Northeast Bioengineering Conference, 2011, pp. 1-2.

[12]. W.Q. Lim, "The discrete shearlet transform: a new directional transform and compactly supported shearlet frames", IEEE Transactions on Image Processing, vol. 19, no. 5, 2010, pp. 1166-1180.

[13]. A. Marcano-Cedeño, J. Quintanilla-Domínguez, M. G. Cortina-Januchs and D. Andina, "Feature selection using sequential forward selection and classification applying artificial metaplasticity neural network," 36th annual conference on IEEE industrial electronics society, 2010, pp. 2845-2850.

[14]. SP.Maniraj and P. Sardarmaran, "Classification of dermoscopic images using soft computing techniques," Neural Computing and Applications, vol. 33, no .19, 2021, pp. 13015-13026.

[15]. Database download link: https://ieee-dataport.org/open-access/childhood-medulloblastoma-microscopic-images.